

Evidence for $f_0(980)f_0(980)$ production in χ_{c0} decays

M. Ablikim¹, J. Z. Bai¹, Y. Ban¹⁰, J. G. Bian¹, X. Cai¹, J. F. Chang¹, H. F. Chen¹⁶, H. S. Chen¹, H. X. Chen¹, J. C. Chen¹, Jin Chen¹, Jun Chen⁶, M. L. Chen¹, Y. B. Chen¹, S. P. Chi², Y. P. Chu¹, X. Z. Cui¹, H. L. Dai¹, Y. S. Dai¹⁸, Z. Y. Deng¹, L. Y. Dong¹, S. X. Du¹, Z. Z. Du¹, J. Fang¹, S. S. Fang², C. D. Fu¹, H. Y. Fu¹, C. S. Gao¹, Y. N. Gao¹⁴, M. Y. Gong¹, W. X. Gong¹, S. D. Gu¹, Y. N. Guo¹, Y. Q. Guo¹, Z. J. Guo¹⁵, F. A. Harris¹⁵, K. L. He¹, M. He¹¹, X. He¹, Y. K. Heng¹, H. M. Hu¹, T. Hu¹, G. S. Huang^{1†}, L. Huang⁶, X. P. Huang¹, X. B. Ji¹, Q. Y. Jia¹⁰, C. H. Jiang¹, X. S. Jiang¹, D. P. Jin¹, S. Jin¹, Y. Jin¹, Y. F. Lai¹, F. Li¹, G. Li¹, H. B. Li¹, H. H. Li¹, J. Li¹, J. C. Li¹, Q. J. Li¹, R. B. Li¹, R. Y. Li¹, S. M. Li¹, W. G. Li¹, X. L. Li⁷, X. Q. Li⁹, X. S. Li¹⁴, Y. F. Liang¹³, H. B. Liao⁵, C. X. Liu¹, F. Liu⁵, Fang Liu¹⁶, H. M. Liu¹, J. B. Liu¹, J. P. Liu¹⁷, R. G. Liu¹, Z. A. Liu¹, Z. X. Liu¹, F. Lu¹, G. R. Lu⁴, J. G. Lu¹, C. L. Luo⁸, X. L. Luo¹, F. C. Ma⁷, J. M. Ma¹, L. L. Ma¹¹, Q. M. Ma¹, X. Y. Ma¹, Z. P. Mao¹, X. H. Mo¹, J. Nie¹, Z. D. Nie¹, S. L. Olsen¹⁵, H. P. Peng¹⁶, N. D. Qi¹, C. D. Qian¹², H. Qin⁸, J. F. Qiu¹, Z. Y. Ren¹, G. Rong¹, L. Y. Shan¹, L. Shang¹, D. L. Shen¹, X. Y. Shen¹, H. Y. Sheng¹, F. Shi¹, X. Shi¹⁰, H. S. Sun¹, S. S. Sun¹⁶, Y. Z. Sun¹, Z. J. Sun¹, X. Tang¹, N. Tao¹⁶, Y. R. Tian¹⁴, G. L. Tong¹, G. S. Varner¹⁵, D. Y. Wang¹, J. Z. Wang¹, K. Wang¹⁶, L. Wang¹, L. S. Wang¹, M. Wang¹, P. Wang¹, P. L. Wang¹, S. Z. Wang¹, W. F. Wang¹, Y. F. Wang¹, Zhe Wang¹, Z. Wang¹, Zheng Wang¹, Z. Y. Wang¹, C. L. Wei¹, D. H. Wei³, N. Wu¹, Y. M. Wu¹, X. M. Xia¹, X. X. Xie¹, B. Xin⁷, G. F. Xu¹, H. Xu¹, Y. Xu¹, S. T. Xue¹, M. L. Yan¹⁶, F. Yang⁹, H. X. Yang¹, J. Yang¹⁶, S. D. Yang¹, Y. X. Yang³, M. Ye¹, M. H. Ye², Y. X. Ye¹⁶, L. H. Yi⁶, Z. Y. Yi¹, C. S. Yu¹, G. W. Yu¹, C. Z. Yuan¹, J. M. Yuan¹, Y. Yuan¹, Q. Yue¹, S. L. Zang¹, Yu Zeng¹, Y. Zeng⁶, B. X. Zhang¹, B. Y. Zhang¹, C. C. Zhang¹, D. H. Zhang¹, H. Y. Zhang¹, J. Zhang¹, J. Y. Zhang¹, J. W. Zhang¹, L. S. Zhang¹, Q. J. Zhang¹, S. Q. Zhang¹, X. M. Zhang¹, X. Y. Zhang¹¹, Y. J. Zhang¹⁰, Y. Y. Zhang¹, Yiyun Zhang¹³, Z. P. Zhang¹⁶, Z. Q. Zhang⁴, D. X. Zhao¹, J. B. Zhao¹, J. W. Zhao¹, M. G. Zhao⁹, P. P. Zhao¹, W. R. Zhao¹, X. J. Zhao¹, Y. B. Zhao¹, Z. G. Zhao^{1*}, H. Q. Zheng¹⁰, J. P. Zheng¹, L. S. Zheng¹, Z. P. Zheng¹, X. C. Zhong¹, B. Q. Zhou¹, G. M. Zhou¹, L. Zhou¹, N. F. Zhou¹, K. J. Zhu¹, Q. M. Zhu¹, Y. C. Zhu¹, Y. S. Zhu¹, Yingchun Zhu¹, Z. A. Zhu¹, B. A. Zhuang¹, B. S. Zou¹.

(BES Collaboration)

¹ Institute of High Energy Physics, Beijing 100039, People's Republic of China

² China Center of Advanced Science and Technology, Beijing 100080, People's Republic of China

³ Guangxi Normal University, Guilin 541004, People's Republic of China

⁴ Henan Normal University, Xinxiang 453002, People's Republic of China

⁵ Huazhong Normal University, Wuhan 430079, People's Republic of China

⁶ Hunan University, Changsha 410082, People's Republic of China

⁷ Liaoning University, Shenyang 110036, People's Republic of China

⁸ Nanjing Normal University, Nanjing 210097, People's Republic of China

⁹ Nankai University, Tianjin 300071, People's Republic of China

¹⁰ Peking University, Beijing 100871, People's Republic of China

¹¹ Shandong University, Jinan 250100, People's Republic of China

¹² Shanghai Jiaotong University, Shanghai 200030, People's Republic of China

¹³ Sichuan University, Chengdu 610064, People's Republic of China

¹⁴ Tsinghua University, Beijing 100084, People's Republic of China

¹⁵ University of Hawaii, Honolulu, HI 96822, USA

¹⁶ University of Science and Technology of China, Hefei 230026, People's Republic of China

¹⁷ Wuhan University, Wuhan 430072, People's Republic of China

¹⁸ Zhejiang University, Hangzhou 310028, People's Republic of China

* Visiting professor to University of Michigan, Ann Arbor, MI 48109, USA

† Current address: Purdue University, West Lafayette, IN 47907, USA

(Dated: June 28, 2021)

Using a sample of 14 million $\psi(2S)$ events accumulated with the BESII detector, evidence for $f_0(980)f_0(980)$ production in χ_{c0} decays is obtained for the first time; the branching ratio is determined to be $\mathcal{B}(\chi_{c0} \rightarrow f_0(980)f_0(980) \rightarrow \pi^+\pi^-\pi^+\pi^-) = (7.6 \pm 1.9 \text{ (stat)} \pm 1.6 \text{ (syst)}) \times 10^{-4}$. The significance of the $f_0(980)$ signal is about 4.6σ .

PACS numbers: 13.25.Gv, 14.40.Cs

I. INTRODUCTION

After thirty years of controversy, the nature of the $f_0(980)$ is still not settled [1]. It has been described as a conventional $q\bar{q}$ meson [2], a “unitarized remnant” of a $q\bar{q}$ state [3], a $K\bar{K}$ molecule [4], a multiquark state [5], or a

glueball [6]. Because of its close proximity to the $K\bar{K}$ threshold and its propensity to decay to $K\bar{K}$, it is difficult to quantify even the mass and width of the $f_0(980)$. To be explicit, the state with a mass of 980 ± 10 MeV and a width somewhere between 40 and 100 MeV [7] straddles the $K\bar{K}$ threshold at 990 MeV. Many arguments favoring or disfavoring the above assignments depend on the width or pole position of the $f_0(980)$.

A novel measurement to elucidate the nature of the $f_0(980)$ was suggested by Refs. [8,9]. By determining the radiative decay rate for $\phi \rightarrow f_0(980)\gamma$, one can infer the $s\bar{s}$ content of the f_0 wave function since the rate is proportional to the overlap with the ϕ , a well known $s\bar{s}$ state. The results from CMD2, SND, and KLOE [10] reveal a much higher branching ratio for radiative $\phi \rightarrow \gamma f_0$ decay than that expected for the $q\bar{q}$ meson or $K\bar{K}$ molecule interpretations. It seems that these data add weight to the idea that the $f_0(980)$ is a compact $q\bar{q}\bar{q}q$ state with an extended meson-meson cloud ‘molecular’ tail [11]. However, at present the interpretation about the nature of the $f_0(980)$ is still open [7], and more experimental results are needed to clarify it.

In this paper, we report on the analysis of $\pi^+\pi^-\pi^+\pi^-$ final states from χ_{c0} decays using a sample of 14 million $\psi(2S)$ events accumulated with the BESII detector. Evidence for $f_0(980)f_0(980)$ production from χ_{c0} decays is obtained for the first time.

II. BES DETECTOR

BESII is a large solid-angle magnetic spectrometer that is described in detail in Ref. [12]. Charged particle momenta are determined with a resolution of $\sigma_p/p = 1.78\%\sqrt{1+p^2}$ (p in GeV/ c) in a 40-layer cylindrical drift chamber (MDC). Particle identification is accomplished by specific ionization (dE/dx) measurements in the drift chamber and time-of-flight (TOF) measurements in a barrel-like array of 48 scintillation counters. The dE/dx resolution is $\sigma_{dE/dx} = 8.0\%$; the TOF resolution is $\sigma_{TOF} = 180$ ps for Bhabha events. Outside of the time-of-flight counters is a 12-radiation-length barrel shower counter (BSC) comprised of gas proportional tubes interleaved with lead sheets. The BSC measures the energies of photons with a resolution of $\sigma_E/E \simeq 21\%/\sqrt{E}$ (E in GeV). Outside the solenoidal coil, which provides a 0.4 Tesla magnetic field over the tracking volume, is an iron flux return that is instrumented with three double layers of counters that are used to identify muons.

In this analysis, a GEANT3 based Monte Carlo simulation package (SIMBES) with detailed consideration of detector performance (such as dead electronic channels) is used. The consistency between data and Monte Carlo has been checked in many high purity physics channels, and the agreement is quite reasonable.

III. EVENT SELECTION

The selection criteria used in this analysis are similar to those of Ref. [13]; the main difference between them is that no particle identification is imposed here in order to increase the selection efficiency.

A. Photon Identification

A neutral cluster is considered to be a photon candidate when the angle between the nearest charged track and the cluster is greater than 15° , the first hit is in the beginning 6 radiation lengths, and the difference between the angle of the cluster development direction in the BSC and the photon emission direction is less than 30° . The photon candidate with the largest energy deposit in the BSC is treated as the photon radiated from the $\psi(2S)$ and used in a four-constraint kinematic fit to the hypothesis $\psi(2S) \rightarrow \gamma\pi^+\pi^-\pi^+\pi^-$.

B. Charged Particle Identification

Each charged track is required to be well fit to a three-dimensional helix using the MDC information, be in the polar angle region $|\cos\theta_{MDC}| < 0.80$, and have the point of closest approach of the track to the beam axis be within 2 cm of the beam and within 20 cm of the center of the interaction region along the beam line.

C. Event Selection Criteria

The candidate events are required to satisfy the following selection criteria:

1. The number of charged tracks is required to be four with net charge zero.
2. The sum of the momenta of the lowest momentum π^+ and π^- tracks is required to be greater than 650 MeV; this removes contamination from $\psi(2S) \rightarrow \pi^+\pi^- J/\psi$ and some $\rho^0\pi\pi$ events.
3. The χ^2 probability for the four-constraint kinematic fit to the decay hypothesis $\psi(2S) \rightarrow \gamma\pi^+\pi^-\pi^+\pi^-$ is greater than 0.01.

The invariant mass distribution for the $\pi^+\pi^-\pi^+\pi^-$ events that survive all the selection requirements is shown in Fig. 1. There are clear peaks corresponding to the χ_{cJ} states. The highest mass peak corresponds to charged track final states that are kinematically fit with an unassociated photon.

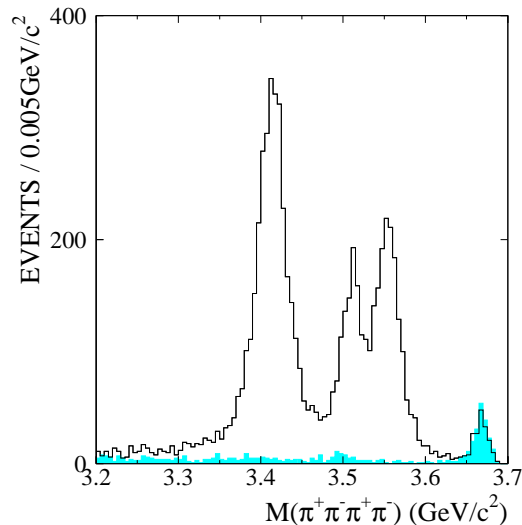


FIG. 1: The $\pi^+\pi^-\pi^+\pi^-$ invariant mass spectrum. The shadow histogram shows the spectrum for Monte Carlo simulated background events.

The distribution of background events in the 4π mass spectrum, determined by Monte Carlo simulation normalized using PDG2004 branching ratios [7], is also shown in Fig. 1. The distribution is flat in the mass range of the χ_{cJ} states, and the background events come mainly from $\psi(2S) \rightarrow \pi^0\pi^+\pi^-\pi^+\pi^-$. The highest mass peak is from $\psi(2S) \rightarrow \pi^+\pi^-\pi^+\pi^-$ and $\psi(2S) \rightarrow \pi^+\pi^-K^+K^-$ events combined with an unassociated photon. The background is very low compared with the strong χ_{cJ} peaks, and its effect will not be considered in the following analysis.

In this analysis, no particle identification is imposed on charged tracks in order to increase the detection efficiency. It is not necessary to distinguish pions from kaons or protons in this channel because the background is not serious, as shown in Fig. 1, and the contamination from events with kaons or protons is rejected effectively by the kinematic fit. The statistics of present data sample is about 20% higher than one using particle identification.

IV. ANALYSIS RESULTS

A. $f_0(980)f_0(980)$ signal

Figure 2 shows scatter plots of $\pi^+\pi^-$ versus $\pi^+\pi^-$ invariant mass [14] for events with $\pi^+\pi^-\pi^+\pi^-$ mass between 3.30 and 3.48 GeV and between 3.53 and 3.60 GeV, and the corresponding projections are shown in Fig. 3 (two entries per event). The clusters of events in the lower left-hand corners of Figs. 2(a) and 2(b) indicate the presence of a $K_S^0K_S^0$ signal under both the χ_{c0} and χ_{c2} peaks. A clear $f_0(980)f_0(980)$ signal can be seen in Fig. 2(a). There are some hints of $\rho^0\rho^0$ and $f_0(1370)f_0(1370)$ (or $f_2(1270)f_2(1270)$) signals in Fig. 2(a) and $\rho^0\rho^0$ but no $f_0(980)f_0(980)$ events in Fig. 2(b). In this paper, we study the $f_0(980)f_0(980)$ in χ_{c0} decays.

For the events in χ_{c0} mass region (from 3.30 to 3.48 GeV) and after requiring that the mass of one of the $\pi^+\pi^-$ pairs lies between 0.88 and 1.04 GeV, the mass distribution of the other $\pi^+\pi^-$ pair is shown in Fig. 4 (two entries per event); there is a strong $f_0(980)$ signal, and its line shape is similar to other experiments [7]. From a Monte

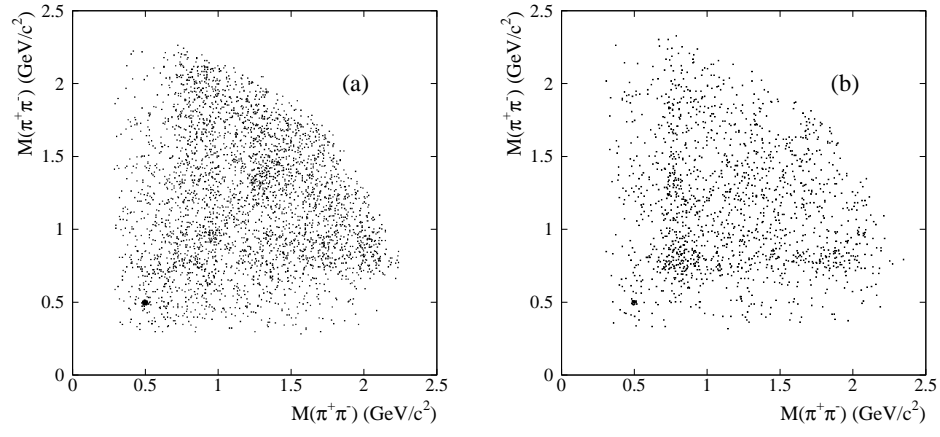


FIG. 2: Scatter plots of $\pi^+\pi^-$ versus $\pi^+\pi^-\pi^+\pi^-$ invariant mass for selected $\gamma\pi^+\pi^-\pi^+\pi^-$ events with $\pi^+\pi^-\pi^+\pi^-$ mass in (a) the χ_{c0} and (b) the χ_{c2} mass regions.

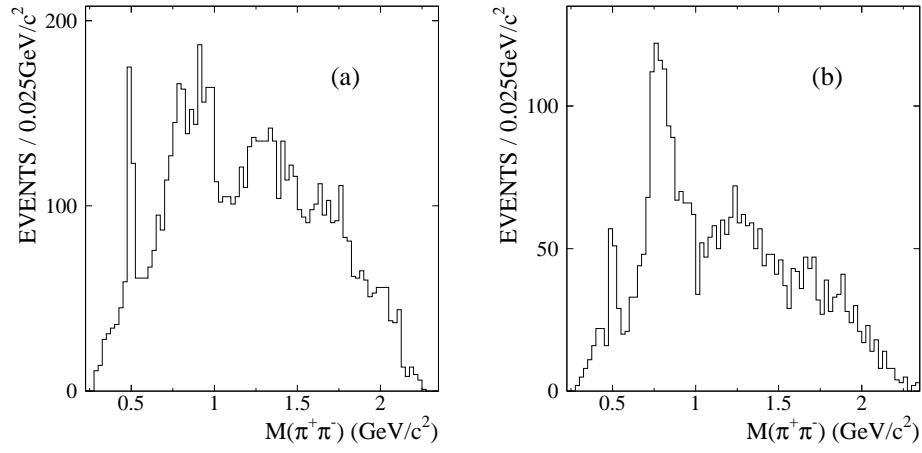


FIG. 3: Projections of $\pi^+\pi^-$ invariant mass under the (a) χ_{c0} and (b) χ_{c2} peaks (two entries per event).

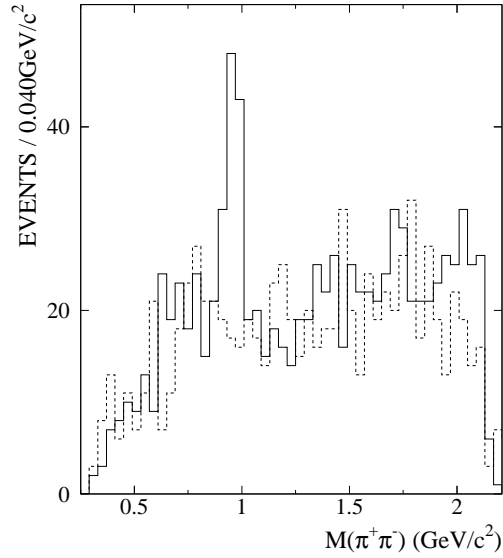


FIG. 4: Plot of $\pi^+\pi^-$ mass recoiling against the $f_0(980)$ ($0.88 \text{ GeV} < m_{\pi^+\pi^-} < 1.04 \text{ GeV}$) for events in the χ_{c0} mass region (two entries per event), where the dashed line histogram indicates a rough estimation of background determined from sidebands.

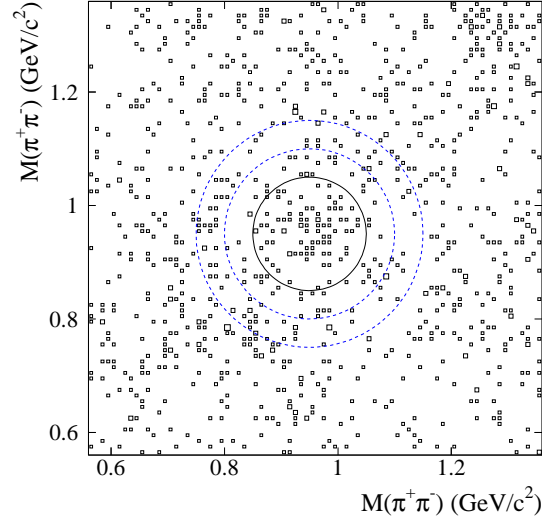


FIG. 5: Scatter plot of $\pi^+\pi^-$ versus $\pi^+\pi^-$ invariant mass in the $f_0(980)$ region for χ_{c0} candidate events, showing the definition of signal and background regions.

Carlo simulation, the background in the $f_0(980)$ region is mainly from processes such as $\psi(2S) \rightarrow \gamma\chi_{c0}$, $\chi_{c0} \rightarrow a_1(1260)\pi$, $a_1(1260) \rightarrow \rho\pi$.

Note that the background estimation in Fig. 4 using sidebands (0.76 - 0.84 GeV and 1.08 - 1.16 GeV) is rough. In this paper, the number of $f_0(980)f_0(980)$ events and the corresponding background are estimated from the scatter plot of $\pi^+\pi^-$ versus $\pi^+\pi^-$ invariant masses, as shown in Fig. 5. This method gives more accurate determinations of the $f_0(980)$ signal and background. The signal region is shown in Fig. 5 as a circle centered at (0.960, 0.960) GeV and with a radius of 80 MeV, and the background is estimated from the events between two circles with radii of 120 MeV and 160 MeV. There are 65 and 51 events in the signal and background regions, respectively. So the number of $f_0(980)f_0(980)$ events is estimated to be $65 - 51/1.75 = 35.9 \pm 9.0$, where 1.75 is the normalization factor – the ratio of the area of background region to that of the signal region. The $\pi^+\pi^-$ mass range we adopt is shifted from the $f_0(980)$ central mass value of 980 MeV because of the asymmetric character of its mass spectrum. We obtain the signal significance of the $f_0(980)f_0(980)$ of 4.6σ using the method described in Ref. [15].

B. Monte Carlo simulation

A Monte Carlo simulation is used to determine the detection efficiency. The angular distribution of the emitted photon in the process $\psi(2S) \rightarrow \gamma\chi_{c0}$ is taken into account [16]. The $f_0(980)$ is generated with the usual Flatté formula [17, 18]:

$$f = \frac{1}{M^2 - s - iM(g_1\rho_1 + g_2\rho_2)},$$

where $\rho_{1,2}$ are the phase space factors for the $\pi\pi$ and $K\bar{K}$ channels, $\rho_i(s) = \sqrt{1 - m_i^2/4s}$, and $g_{1,2}$ are squares of coupling constants to the two channels. For the $K\bar{K}$ channel, m^2 is taken as the average of the K^0 and K^\pm masses, and the algebraic expression for ρ_2 is extended analytically below the $K\bar{K}$ threshold. In the simulation, the parameters used are those of Ref. [18]: $M = 0.9535$, $g_1 = 0.1108$, $g_2 = 0.4229$ GeV.

C. Branching fraction results

The efficiency is determined using 100,000 Monte Carlo simulated events that are passed through the same selection as the data events; the efficiency is estimated to be $\epsilon = (3.92 \pm 0.07)\%$, where the error is the statistical error of the Monte Carlo sample. Note that for this estimation, the events in the background region are subtracted from the events in the signal region, similar to the treatment of data.

Using numbers from above, the branching ratio of $\psi(2S) \rightarrow \gamma\chi_{c0}$, $\chi_{c0} \rightarrow f_0(980)f_0(980) \rightarrow \pi^+\pi^-\pi^+\pi^-$ is

$$\mathcal{B}(\psi(2S) \rightarrow \gamma\chi_{c0} \rightarrow \gamma f_0(980)f_0(980) \rightarrow \gamma\pi^+\pi^-\pi^+\pi^-) = (6.54 \pm 1.64) \times 10^{-5},$$

where the error is statistical.

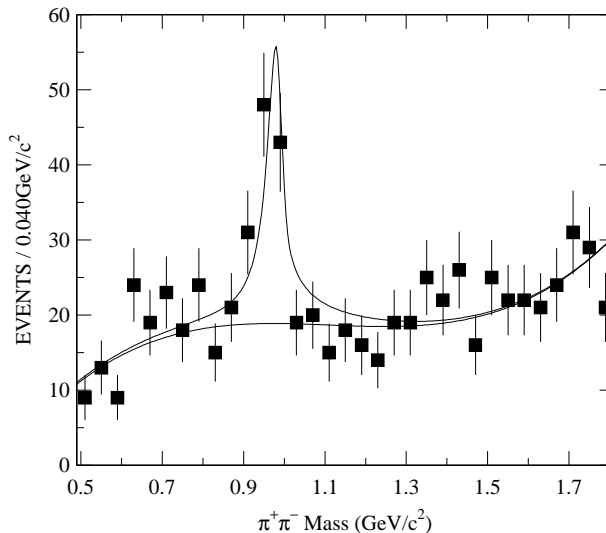


FIG. 6: A fit to the $\pi^+\pi^-$ mass recoiling against the $f_0(980)$ ($0.88 \text{ GeV} < m_{\pi^+\pi^-} < 1.04 \text{ GeV}$) for events in the χ_{c0} mass region (two entries per event).

As a cross-check, a fit to the projected $\pi^+\pi^-$ mass distribution between 0.49 and 1.81 GeV with the Flatté parameters of the $f_0(980)$ fixed to the solution of Ref. [18] plus a polynomial background yields 84.8 ± 18.4 events for the $f_0(980)$ signal, as shown in Fig. 6 (two entries per event). From the results of this fit, we determine the branching ratio

$$\mathcal{B}(\psi(2S) \rightarrow \gamma\chi_{c0} \rightarrow \gamma f_0(980)f_0(980) \rightarrow \gamma\pi^+\pi^-\pi^+\pi^-) = (4.54 \pm 0.98) \times 10^{-5},$$

where the detection efficiency is 13.34% (two entries per event). Because of the low statistics and the relatively high backgrounds, as well as the lack of information from the coupled $K\bar{K}$ channel, a free fit to the parameters M , g_1 , and g_2 is difficult. The branching ratio values determined by these two methods agree to about one sigma.

D. Systematic errors

The systematic errors in the branching ratio measurement associated with the efficiency are determined by comparing $\psi(2S)$ data and Monte Carlo simulation for very clean decay channels, such as $\psi(2S) \rightarrow \pi^+\pi^-J/\psi$, which allows the determination of systematic errors associated with the MDC tracking, kinematic fitting, and the photon identification [19]. Other sources of systematic error come from the uncertainties of the number of $\psi(2S)$ events [20], the parameters of the $f_0(980)$, the definition of background region, the χ_{c0} and $f_0(980)$ mass resolutions, etc.

1. Parameters of the $f_0(980)$

The parameters of the $f_0(980)$ are still uncertain, and different descriptions of the $f_0(980)$ in the simulation result in different efficiencies. Besides the solution of Ref. [18], we also consider the measurements of some recent experiments such as E791, GAMS and WA102 [21-23], where a Breit-Wigner description with the width varying from 44 to 80 MeV was used for the $f_0(980)$. We determine the change both by using the solutions of Refs. [21-23] and by varying g_1 in Ref. [18] from 0.1108 GeV to 0.090 GeV and 0.130 GeV while keeping the ratio g_2/g_1 fixed. The largest change is about 16%, which is used for the systematic error due to this uncertainty.

2. Different background regions

In this paper, we estimate the background using the region between circles with radii 120 MeV and 160 MeV about (0.960, 0.960) GeV, as shown in Fig. 5. We test two other different background definitions by changing the radii of the two circles to 100 and 150 MeV and 120 and 180 MeV. The biggest change is about 5%, which is taken as the systematic error.

3. χ_{c0} and $f_0(980)$ mass resolutions

Differences between data and Monte Carlo mass resolutions for the χ_{c0} and $f_0(980)$ also cause systematic uncertainties in the determination of the branching ratio of $\chi_{c0} \rightarrow f_0(980)f_0(980)$. From a study, we find that the difference for the χ_{c0} is about 1 MeV, so we change the window of χ_{c0} to $[3.300 + 0.005, 3.480 - 0.005]$ GeV and $[3.300 - 0.005, 3.480 + 0.005]$ GeV, and estimate the effect on the branching ratio. Such changes result in less than a 1% variation in the efficiency, and the effect of the difference in the mass resolutions of the $f_0(980)$ is even smaller. By varying the width of χ_{c0} by 1σ of its error, 0.8 MeV, there is almost no change on the detection efficiency. We include a 1% systematic error for the sum of these uncertainties.

Table I lists the systematic errors from all sources, and adding them in quadrature, the total systematic error, 20%, is obtained. The resulting branching ratio is

$$\mathcal{B}(\psi(2S) \rightarrow \gamma\chi_{c0} \rightarrow \gamma f_0(980)f_0(980) \rightarrow \gamma\pi^+\pi^-\pi^+\pi^-) = (6.5 \pm 1.6 \pm 1.3) \times 10^{-5},$$

and finally using the PDG2004 average value and error for $\mathcal{B}(\psi(2S) \rightarrow \gamma\chi_{c0})$ [7], we obtain

$$\mathcal{B}(\chi_{c0} \rightarrow f_0(980)f_0(980) \rightarrow \pi^+\pi^-\pi^+\pi^-) = (7.6 \pm 1.9 \text{ (stat)} \pm 1.6 \text{ (syst)}) \times 10^{-4}.$$

TABLE I: Summary of systematic errors in the branching ratio calculation of $\mathcal{B}(\psi(2S) \rightarrow \gamma\chi_{c0} \rightarrow \gamma f_0(980)f_0(980) \rightarrow \gamma\pi^+\pi^-\pi^+\pi^-)$.

Source	Relative systematic error
MDC tracking	8%
Kinematic fit	6%
Photon ID efficiency	2%
$\psi(2S)$ number	4%
Efficiency estimation	16%
Definition of background	5%
Mass resolutions	1%
Total	20%

V. SUMMARY

Evidence for $f_0(980)f_0(980)$ production from χ_{c0} decays is obtained for the first time with a significance of about 4.6σ , and the branching ratio is determined to be $\mathcal{B}(\chi_{c0} \rightarrow f_0(980)f_0(980) \rightarrow \pi^+\pi^-\pi^+\pi^-) = (7.6 \pm 1.9 \text{ (stat)} \pm 1.6 \text{ (syst)}) \times 10^{-4}$. This may help in understanding the nature of $f_0(980)$.

VI. ACKNOWLEDGMENTS

The BES collaboration thanks the staff of the BEPC for their hard efforts. This work is supported in part by the National Natural Science Foundation of China under contracts Nos. 19991480, 10225524, 10225525, the Chinese Academy of Sciences under contract No. KJ 95T-03, the 100 Talents Program of CAS under Contract Nos. U-11, U-24, U-25, and the Knowledge Innovation Project of CAS under Contract Nos. U-602, U-34 (IHEP); by the National

Natural Science Foundation of China under Contract No.10175060 (USTC); and by the Department of Energy under Contract No. DE-FG03-94ER40833 (U Hawaii).

-
- [1] For general reviews, see S. Godfrey and J. Napolitano, Rev. Mod. Phys. **71** (1999) 1411; C. Amsler and N. Törnqvist, Phys. Rept. **389** (2004) 61.
 - [2] D. Morgan, Phys. Lett. **B51** (1974) 71.
 - [3] N. Törnqvist, Phys. Rev. Lett. **49** (1982) 624.
 - [4] J. Weinstein and N. Isgur, Phys. Rev. Lett. **48** (1982) 659; Phys. Rev. **D27** (1983) 588; *ibid.* **D41** (1990) 2236.
 - [5] R.L. Jaffe, Phys. Rev. **D15** (1977) 267; N.N. Achasov and G.N. Shestakov, Z. Phys. **C41** (1988) 309.
 - [6] D. Robson, Nucl. Phys. **B130** (1977) 328.
 - [7] S. Eidelman *et al.* (Particle Data Group), Phys. Lett. **B592** (2004) 1.
 - [8] F. Close, N. Isgur and S. Kumano, Nucl. Phys. **B389** (1993) 513.
 - [9] N. Achasov and V. Ivanchenko, Nucl. Phys. **B315** (1989) 465.
 - [10] R. Akhmetshin *et al.* (CMD2 Collaboration), Phys. Lett. **B462** (1999) 371; M. Achasov *et al.* (SND Collaboration), *ibid.* **B485** (2000) 349; A. Aloisio *et al.* (KLOE Collaboration), hep-ex/0107024, Phys. Lett. **B537** (2002) 21.
 - [11] F. Close and N. Törnqvist, J. Phys. **G28** (2002) R249.
 - [12] J.Z. Bai *et al.* (BES Collaboration), Nucl. Instrum. Meth. **A458** (2001) 627.
 - [13] J.Z. Bai *et al.* (BES Collaboration), Phys. Rev. **D60** (1999) 072001.
 - [14] One $\pi^+\pi^-$ pair is formed using the highest momentum π^+ and the lowest momentum π^- tracks. The other pair uses the two remaining tracks.
 - [15] S.I. Bityukov, JHEP 0209:060, 2002, Nucl. Instrum. Meth. **A502** (2003) 795.
 - [16] W. Tanenbaum *et al.* (Mark I Collaboration), Phys. Rev. **D17** (1978) 1731; G. Karl, S. Meshkov and J.L. Rosner, *ibid.* **D13** (1976) 1203; M. Oreglia *et al.* (Crystal Ball Collaboration), *ibid.* **D25** (1982) 2259.
 - [17] S. Flatté, Phys. Lett. **B63** (1976) 224.
 - [18] B.S. Zou and D.V. Bugg, Phys. Rev. **D48** (1993) R3948.
 - [19] J.Z. Bai *et al.* (BES Collaboration), Phys. Rev. **D69** (2004) 012003.
 - [20] X.H. Mo *et al.*, High Energy Phys. Nucl. Phys. **28** (2004) 455.
 - [21] E.M. Aitala *et al.* (E791 Collaboration), Phys. Rev. Lett. **86** (2001) 765.
 - [22] R. Bellazzini *et al.* (GAMS Collaboration), Phys. Lett. **B467** (1999) 296.
 - [23] D. Barberis *et al.* (WA102 Collaboration), Phys. Lett. **B453** (1999) 316; *ibid.* **B453** (1999) 325.